The International Journal of Advanced Manufacturing Technology (2024) 132:2877–2888
https://doi.org/10.1007/s00170-024-13481-3

ORIGINAL ARTICLE

Modelling the weld cladding process to predict weld clad position and shape error

Vojtěch Votruba[1] · Tomáš Fornůsek[1] · Tomáš Havlan[1] · Tomáš Kratěna[1] · Jan Smolík[2]

Received: 22 November 2023 / Accepted: 18 March 2024 / Published online: 5 April 2024

Abstract

Wire arc additive manufacturing (WAAM) is one of the most productive metal additive manufacturing methods. One of its most promising applications holds in the manufacturing of difficult-to-cut materials where production costs can be reduced with minimizing the time of machining and total tool costs. To develop a correct WAAM, technological processes for manufacturing complex-shaped components welding torch path corrections and welding power corrections have to be made especially in critical sections such as corners and sharp edges. A predictive mathematical model of the material cladding during the WAAM process has been developed for the purposes of generating an optimal toolpath of the WAAM clads. This predictive mathematical model is simplified to reflect the important physical phenomena in the weld pool but also to optimize computing time. In this paper, the principle of the mathematical model is described, and its functionality is verified by the welding experiments with five different welding power settings. For the initial calibration of the model parameters single straight-line weld clads with 5 different welding power settings (wire feeds) ranging from 5.0 to 8.6 m/min were investigated. 3D scans of these welded samples are used for the verification. With the calibrated simulation model, it was possible to predict the precise shape with a maximum deviation circa 0.20 mm. The start portions of the weld clads seem more complex having the deviation circa 0.30 mm. These are valuable results as the WAAM technology is generally considered to be reasonably rough.

Keywords Wire arc additive manufacturing · Simulation · Toolpath · Cold metal transfer · 3D scanning

1 Introduction

A subtype of metal additive manufacturing (AM) which combines wire as a feedstock and electric arc as a heat source is called wire arc additive manufacturing (WAAM) [1, 2]. High deposition rates and low equipment costs are the main advantages of WAAM over other metal AM methods such as laser metal deposition (LMD) and selective laser melting (SLM) [2]. However precision and possible geometrical complexity of manufactured parts are higher when using LMD or SLM [3]. Manufacturing complex shapes that are not possible to be machined in a conventional way is a suitable application for WAAM, especially when WAAM is combined with milling. Inter-operational milling during the WAAM process greatly increases the precision which otherwise might not be sufficient when using WAAM. So far, our experience shows that manufacturing inner cooling channels in thermally stressed components is the application in which the industrial companies are greatly interested. This type of geometry can be manufactured using hybrid WAAM as it is shown in the paper [4].

Techniques used for WAAM can be further categorized by the type of arc welding process. Three basic techniques are gas tungsten arc welding (GTAW), gas metal arc welding (GMAW), and plasma arc welding (PAW) [5]. According to the current state of the art discussed also in [5, 6], a GMAW modification, known as cold metal transfer (CMT), should be the most effective and suitable method for 5-axis WAAM. Nevertheless, different approaches to the WAAM where only 3-axis motions are used suggest PAW as the optimal method

✉ Vojtěch Votruba
V.Votruba@rcmt.cvut.cz

[1] Department of Production Machines and Equipment (RCMT), Faculty of Mechanical Engineering, Czech Technical University in Prague, Technicka Street 4, 16607, Prague 6, Czech Republic

[2] Department of Production Machines and Equipment (RCMT), Faculty of Mechanical Engineering, Center of Advanced Aerospace Technology, Czech Technical University in Prague, Technicka Street 4, 16607, Prague 6, Czech Republic

[2]. The disadvantages of PAW are most significant when manufacturing complex shapes which is the main reason this research relies on GMAW CMT.

Numerous research papers deal with the simulation of the WAAM process with the majority of them focusing on thermal phenomena (for example [7–9]). However, there are not many published papers about weld clad position error during WAAM. An approach to the weld clad position simulation using the machine learning principle is presented in [10]. Weld clad shape cross-section prediction is presented in [11] where the authors are utilizing neural network algorithms for very precise prediction. However, the study does not deal with the 3D shape of the weld clad including the start and end sections. It is usual that WAAM produces blanks that are further machined [2]. However, increasing the precision of WAAM can save costs spent on further machining and allow the possibility of manufacturing more complex geometrical shapes like the ones mentioned in [12] where the influence of precision of the CAD model on the finish milling process is investigated.

The author's main aim is to improve weld clad position accuracy and predict the shape errors of the clads (particularly the start and the end portions of the weld clads). To increase the position accuracy of the weld clads, it is necessary to study the physical phenomena in the weld pool like metal transfer and forces acting on the metal droplet. From this knowledge, a rather simplified mathematical model of weld cladding was developed because using a full-scale FEM simulation is very demanding on a computing power and also very complex to use [13] where the 6 s of CMT welding process took days of computing time. The simplified mathematical model is designed to predict a portion of weld clad position error. The position error prediction may be further used to generate a corrected WAAM toolpath.

1.1 Analysis of the main physical phenomena affecting the weld clad position

In the CMT welding process, the metal droplet is transferred in the modified (controlled wire retraction movement) short-circuit transfer mode [14, 15]. In addition, welding parameters used in the study (127–176 A, 15,4–17,4 V) correspond to the short-circuit transfer mode as shown in Fig. 1 [16]. During the short-circuit metal transfer, various forces affect the liquid metal droplet [17]. These forces are shown in Fig. 2 [17].

The study [18] shows the shape of the weld pool during WAAM. In Fig. 3, it is clearly visible that the liquid metal solidifies at the distance "behind" the axis of the welding torch. This distance depends on the welding method and welding parameters [18, 19].

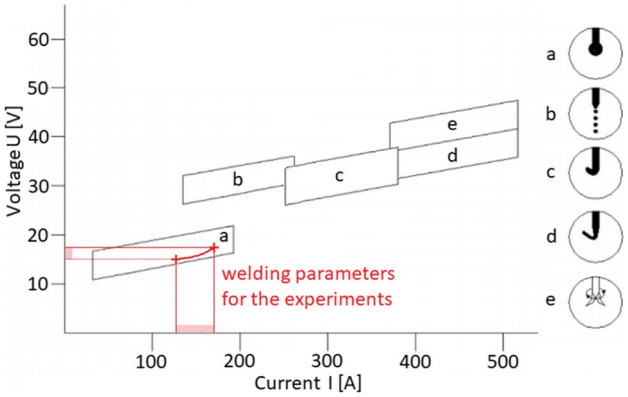

Fig. 1 Metal transfer mode. a — short circuit, b — globular, c — spray, d — streaming, e — streaming rotating [16]

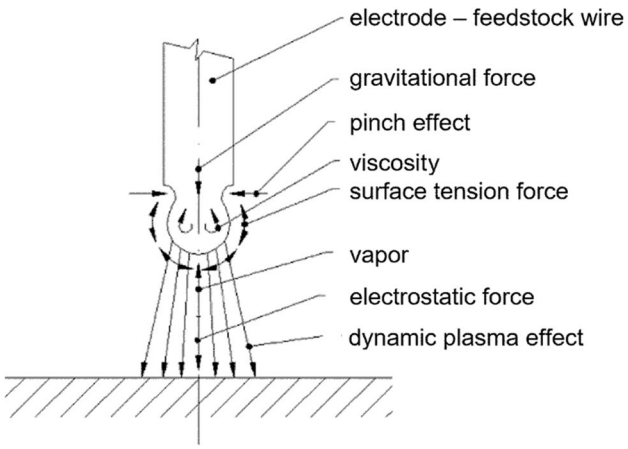

Fig. 2 Forces on the metal droplet during the welding process [17]

2 Design of a mathematical model for predicting weld clad position error

In Fig. 4, the scheme explains the difference between the full-scale FEM simulation [20] and the simplified mathematical model used in this study.

For the simplified mathematical model of WAAM cladding, it is assumed that the welding torch is always normal to the substrate. During welding, the torch is moving only in the plane parallel to the substrate (xy). A preview is shown in Fig. 5. This simplification eliminates most of the forces affecting the liquid metal droplet shown in Fig. 2 as their acting vector is normal to the substrate leaving the surface tension force the only one which affects the XY position. The next phenomenon affecting the XY position of the weld clad is the weld pool length which causes the metal to solidify in a distance "behind" the axis of the welding torch. This can also be seen in Fig. 3.

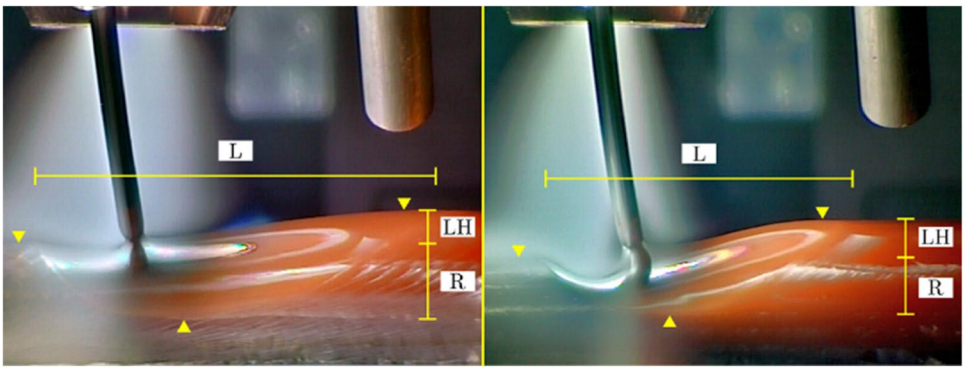

Fig. 3 Weld pool length: left — high welding power, right — low welding power [18]

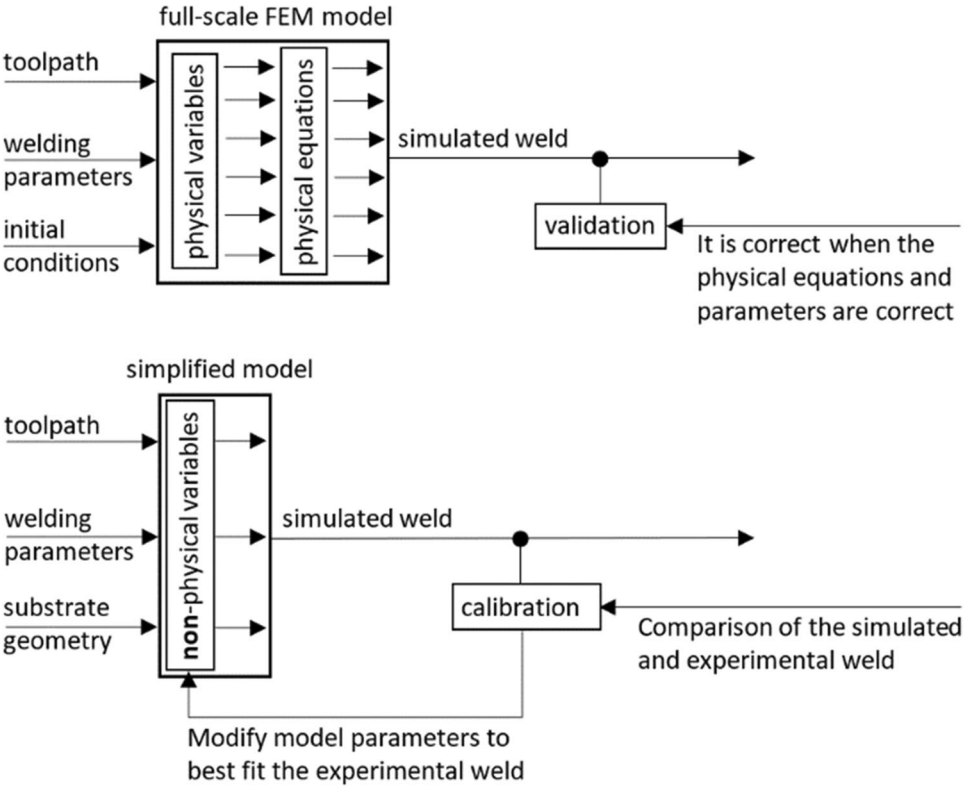

Fig. 4 Scheme of the simplified mathematical model for predicting weld clad position

According to the authors, two phenomena, which are the surface tension force acting on the liquid metal droplet and the weld pool length, are considered to have the main effect on the weld clad position error. These phenomena were incorporated into the simplified mathematical model of weld cladding.

The basic interface of the simplified mathematical model of weld cladding was designed in Matlab software. The substrate is defined by the two-dimensional matrix M (Fig. 6 — left). The two dimensions of matrix M represent the X and Y dimensions in the workspace. Matrix values represent the Z dimension. The shape of the substrate is obtained by creating a surface chart of the M matrix. The 110 × 110 mm substrate is represented by 1100 × 1100 matrix meaning the smallest distinguishable element is 0.1 × 0.1 mm.

In the simulation, the weld clad is created by adding a "droplet element" (Fig. 6 — right) along the defined trajectory. The droplet element is also a two-dimensional matrix, the size of this matrix corresponds to the welding parameters (circa 6 × 6 mm). The "droplet element" matrix is added to substrate matrix M in every step (0.01 s) of the simulation along the defined trajectory. The result of the successive addition is a final matrix describing a weld clad on the substrate. The final shape is obtained by creating a surface chart of the final matrix (Fig. 6 — bottom).

The size and shape of the "droplet element" has to be obtained from the shape of the real weld seam and it is also inspired by the shape of the heat source model for welding [21]. Values of the "droplet element matrix" were

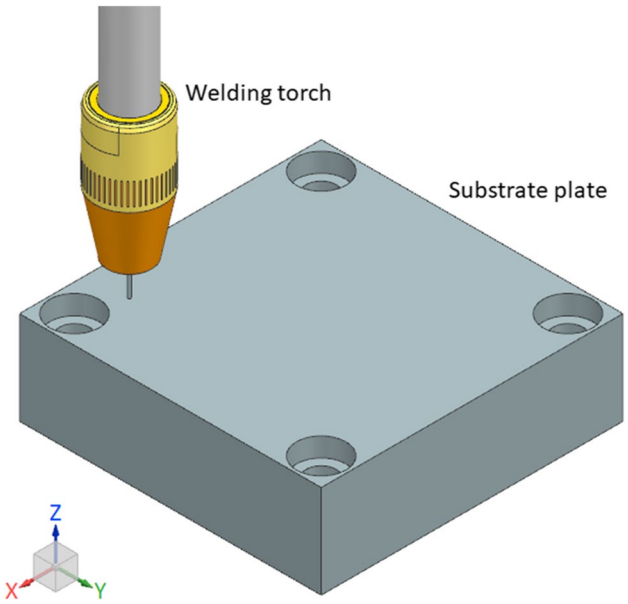

Fig. 5 Considered weld cladding situation

defined in a way that simulated weld seam shape match the experimental weld seam shape.

The deposition process in the simulation is split in two different steps. In the first step, 35% of the volume is cladded exactly along the NC code toolpath. In the second step, 65% of the volume is cladded according to the phenomena known from the physical behavior of the melt pool — these are (i) the effect of the weld pool length and (ii) the surface tension force acting on the liquid metal droplet. This split in the simulated cladding process allows to create weld clads that have almost equal shape as the real weld clads and also as the shape described in [22] where the first step of cladding represents the partial melting of the substrate.

To create a weld clad shape (also used in [23]), shown in Fig. 7, basic parameters for setting the size of the droplet element and simulated cladding are needed to be set in the simulation — see Table 1. The torch speed is not involved by these parameters because it would be redundant for the simulation which works in step-by-step manner. It is assumed that the welding process with a wire feed/power of 6 m/min and torch speed of 0.6 m/min will behave the same as the welding process with a wire feed/power of 10 m/min and torch speed of 1 m/min as the calculated volume of the droplet elements are equal (the equation of continuity applies). However, the width and height of the weld clads will be different.

2.1 Effect of the weld pool length

As shown in Fig. 3, according to the study [16], the length of the weld pool depends on the welding parameters and it is clear that this phenomenon is present in the WAAM process. It was decided that this phenomenon would be incorporated in the mathematical model using a simplification inspired by a "ball pulled on a string." The principle is shown in Fig. 8.

As the weld pool length could not be calculated precisely because it depends on many variables, it is necessary to determine the weld pool length experimentally.

2.2 Surface tension force acting on the liquid metal droplet

Assuming that during welding a substrate is partially melted and a part of metal droplets do not solidify until an emission of the next liquid metal droplet from the electrode happens — this means that the position of the depositing liquid metal droplet is affected by the recently deposited material and the substrate shape. According to these assumptions, a function which scans a close surroundings of an actual droplet deposition was designed. In this area, an XY position of the mass center is calculated. The deposited droplet is then translated in the direction of this mass center vector multiplied by the sF parameter. This simplification is a compensation of a surface tension force acting on the liquid metal droplet effect and it is also explained in Fig. 9.

A simplified mathematical model of the weld cladding contains parameters which are dependent on the welding parameters and materials used but their values are unknown. To calibrate this simplified mathematical model, an experimental weld clads should be made. From the comparison of the experimental and the simulated weld clads positions above mentioned mathematical model parameters can be obtained. An overview of weld pool parameters used in the simplified mathematical model of weld cladding is shown in Table 2. The scheme of an experimental calibration process is shown in Fig. 10.

3 Experimental setup

The experimental welds were manufactured on the 5-axis welding machine equipped with Fronius TPS 320i welding source. For the experiments, only 3-axis operations were used. Toolpath deviations (because of the actuators and interpolation control) could be significant when using serial kinematics (e.g., industrial robot) [24]. However, when using standard CNC kinematics and actuators, and if the toolpath is trivial, these deviations are much smaller. Complete welding equipment is shown in Fig. 11. Substrate material for welding was S235JRG1 (EN10025) 110 × 110 × 40 mm plates. As a welding wire, Voestalpine Böhler X70-IG Ø 1 mm was used together with a shielding gas mixture from Messer — 18% CO_2 in argon. For the 1st set of experiments, five different settings of welding power were used to prove

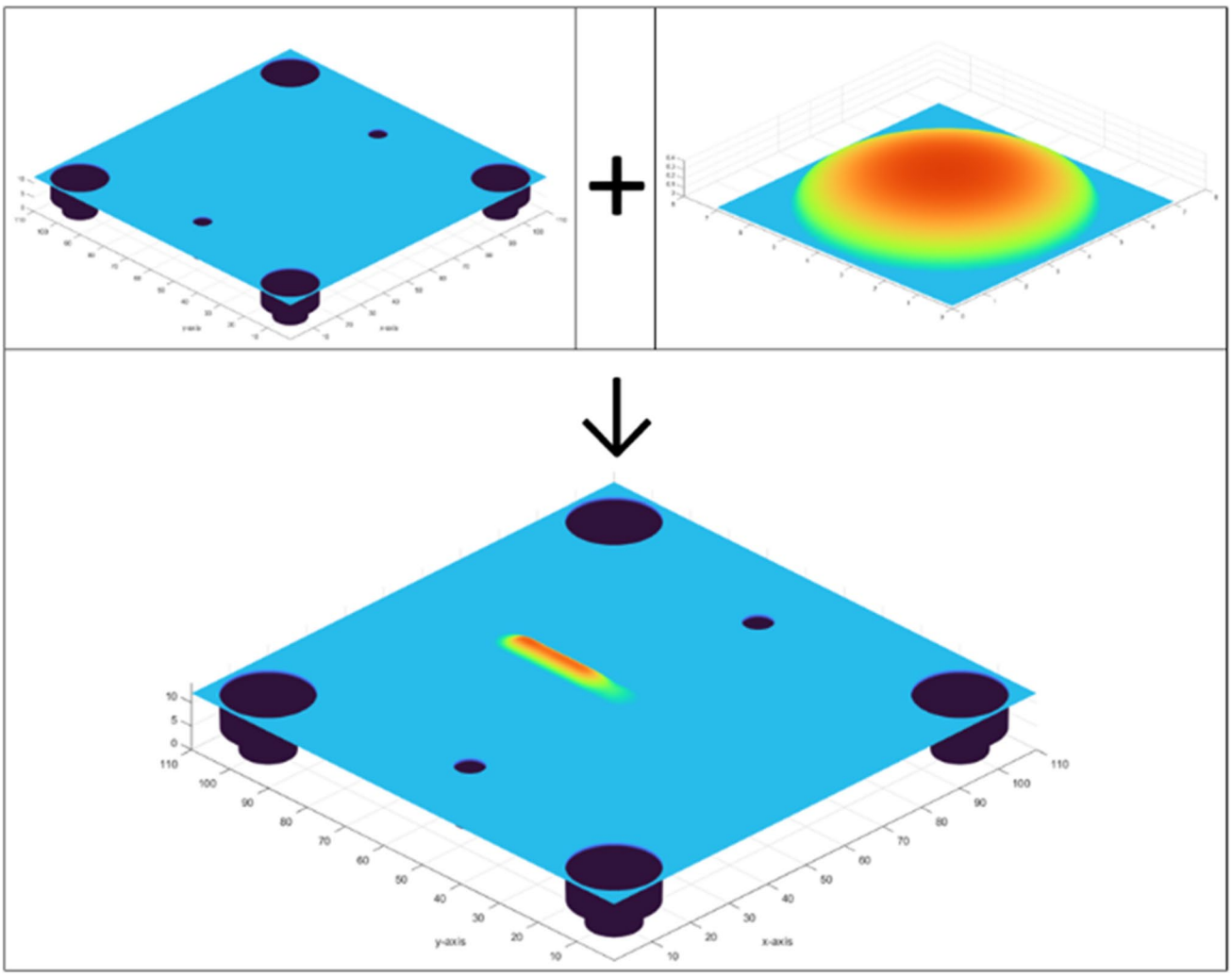

Fig. 6 Interface of the mathematical model shown in Matlab representing one weld clad on the substrate plate

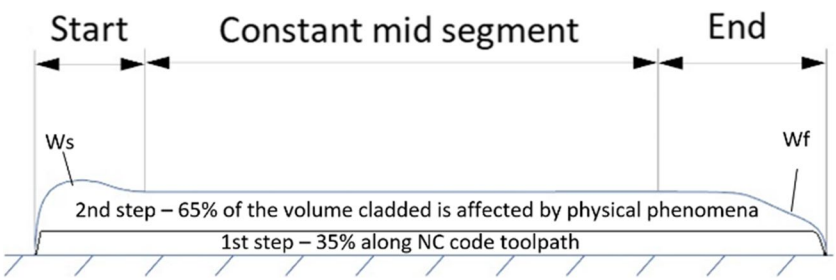

Fig. 7 The split of the cladding process into two steps

that the model is functional for different welding parameters. Welding parameters are shown in Table 3.

For 3D scanning (which was also used in [25]) of experimental welds, an optical 3D scanner Atos Capsule by GOM was used (shown in Fig. 12). The output from the GOM software is an STL file. This STL file is loaded into the mathematical model using a Matlab function called "stlread." When the origin and the scale are set correctly, it is possible to project both simulated (Fig. 13) and experimental welds in one surface chart to detect the deviation between them. For easier evaluation of the deviation between simulated and experimental weld, a Rhinoceros software was used. Rhinoceros has a function to calculate the chart of deviation between two surfaces, so it is not necessary to program this function as a script in Matlab.

Table 1 Basic parameters of the simplified mathematical model of weld cladding

Parameter name	Explanation
Dw [mm]	Feedstock wire diameter used in the welding process
s [m/min]	Wire feed speed which corresponds to the welding power. This is internally measured by Fronius unit. Real wire feed speed differs from the set value
rw [mm]	The width of the weld clad has to be obtained experimentally. The height of the weld clad is then calculated from the total wire feedstock input (Dw and s)
H [vector]	Torch toolpath vector. This can be obtained from the NC code
Ws [%]	Volume increases in the first second of the welding process caused by cladded material before the torch starts moving. Weld initiation process. This has to be obtained experimentally
Wf [-]	Number of droplet elements missing in the end of the weld clad when the torch finishes the movement. Weld termination process. This has to be obtained experimentally

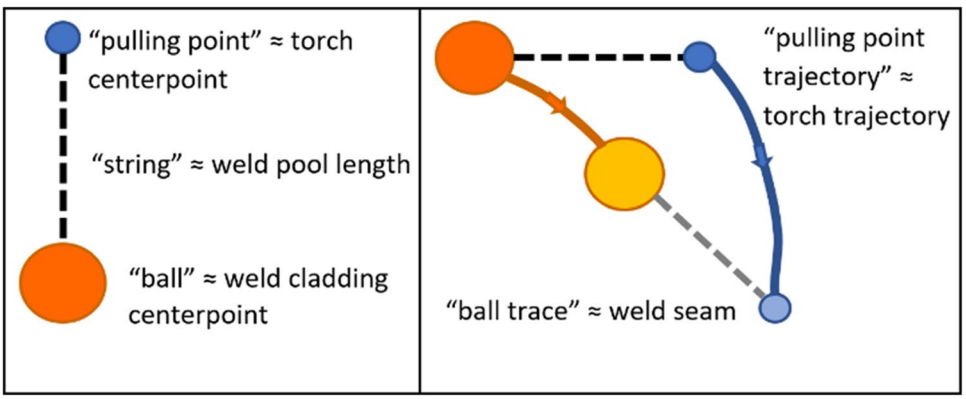

Fig. 8 Model for simulating the weld pool length phenomenon

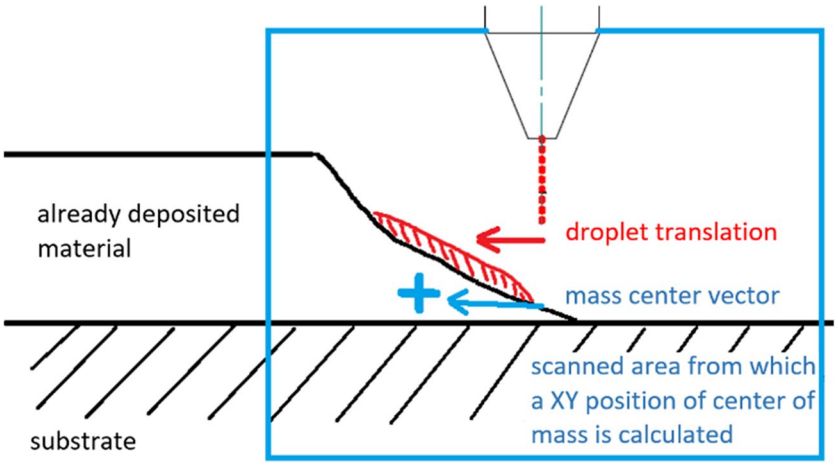

Fig. 9 Model for simulating surface tension force acting on a liquid metal droplet in the weld pool

The purpose of this set of 3 experimental samples is to obtain the basic parameters to create a simple line weld clad. Different welding power settings were used in a way that for each weld clad, it is possible to find the optimal size of the droplet element. For optimal settings of the **D**, **sF,** and **So**, **sH** further experiments have to be conducted. It was necessary to add features for establishing correct zero points of the coordinate systems, otherwise, the measurement accuracy would be unsatisfying. Also, the substrate plates have to be a minimum of 20 mm thick otherwise the plate would be heat deformed which disrupts measurement accuracy.

A set of three experimental samples were manufactured. Each sample contains 5 weld clads with the same welding strategy but different welding power — Fig. 14. The samples were sanded after welding which made them suitable for 3D scanning.

Table 2 Weld pool parameters of the simplified mathematical model of weld cladding

Parameter	The meaning in the mathematical model	The meaning in the real welding process
D [mm]	The length of the "string" guide between torch centerpoint and weld cladding centerpoint	The distance between torch centerpoint and the spot where liquid metal solidifies
sF [-]	Correction factor which is used to calculate translation of deposited droplet along the vector directed to the center of mass of the scanned area	Defines the total effect of surface tension force acting on the deposited droplet
So a sH [mm]	Define a size of the scanned area in which an actual center of mass is calculated	Defines a size of the area where the substrate and deposited material are partially melted thus surface tension force is in effect

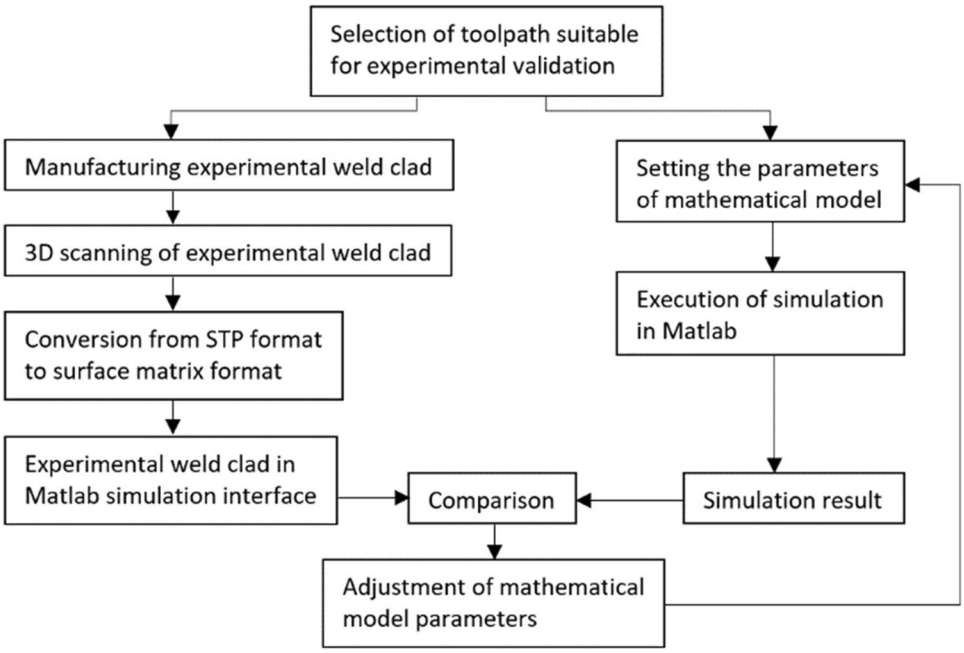

Fig. 10 The scheme of the calibration process

Fig. 11 Experimental WAAM machine setup

Table 3 Welding parameters for experimental clads

Welding strategy	MIG CMT
Wire feed [m/min]	5.0 – 5.9 – 6.8 – 7.7 – 8.6
Torch travel speed [m/min]	0.6
Current [A]	127 – 146 – 155 – 162 – 176
Voltage [V]	15.4 – 16.4 – 16.8 – 17.1 – 17.4
Shielding gas flow [l/min]	15

Two 6 mm holes for center pins were used as an establishment of the XY of the coordinate system. The top and bottom surfaces were face-milled. The top surface works as Z level establishment of the coordinate system. The side walls of the substrate plate were not machined and neither involved in the 3D scan because their geometry is not accurate — Fig. 15.

4 Results and discussion

4.1 Calibration procedure

After 3 samples were 3D scanned and converted to the STL file format, it was possible to start the calibration of the basic model parameters of the simplified model of weld cladding in Matlab. To correctly specify the deviation between simulated and real/3D scanned weld clad, Rhinoceros 7 software function called surface deviation was used. Basic

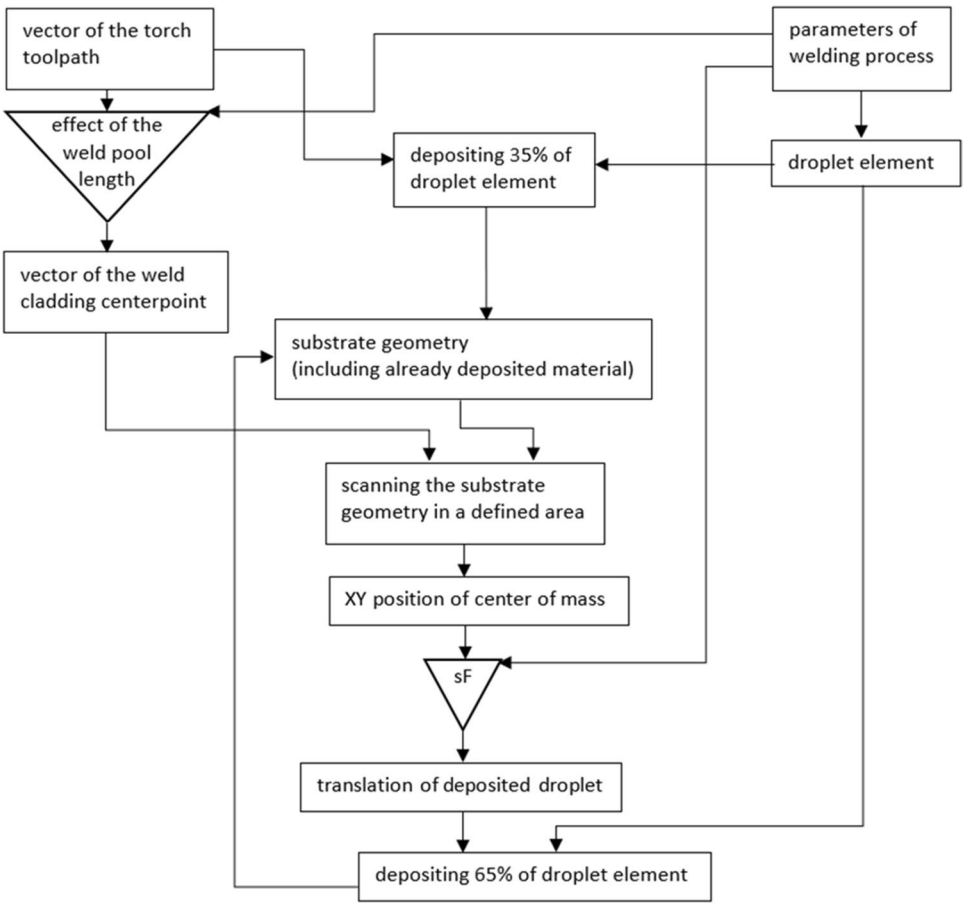

Fig. 12 Complete diagram of the model functionality

Fig. 13 Atos Capsule by GOM (left) is able to create an STL model (right) of the experimental sample

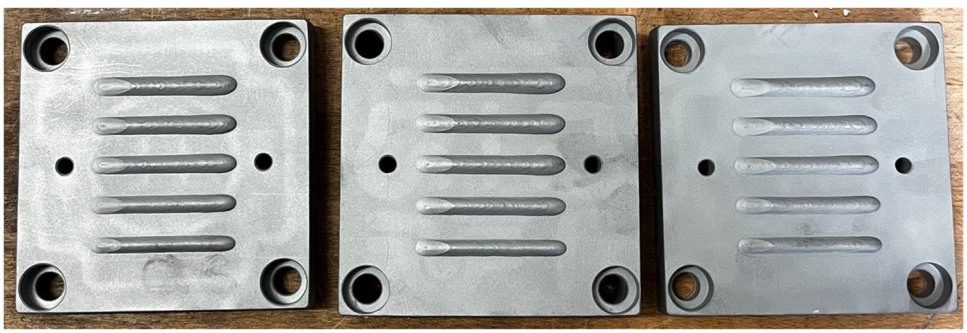

Fig. 14 Experimental weld clads samples — sanded for 3D scanning

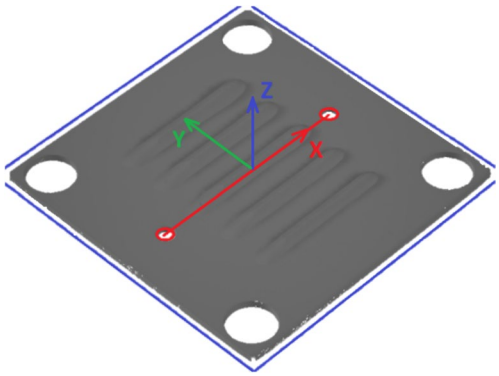

Fig. 15 Coordinate system of the samples STL file obtained from 3D scanning

model parameters were obtained/calibrated by the following procedure.

4.1.1 Dw

Voestalpine Böhler X70-IG Ø 1 mm was used.

4.1.2 s

Real wire feed internally measured by Fronius welding unit. The measured wire feed differs from the set wire feed. It is necessary to use the measured average values rather than the set ones so the simulation fits the experiment — Table 4. The measured wire feed values are noisy, so the standard deviation for each weld clad measured values from all 3 samples are also included in Table 4.

4.1.3 rw

The width of the weld clads has been measured from the STL files using Rhinoceros 7 software.

4.1.4 Ws and Wf

Both of these parameters have been obtained by manual calibration using the Rhinoceros 7 software. The goal was so the simulated weld clad shape to be fitted to overlay with the 3D scanned weld clad shape as ideally as possible.

5 Calibration results

Using the experiments, it was possible to calibrate the simplified model of weld cladding for 5 different welding powers. To calibrate the simplified model for different materials or welding strategies, more experiments would have to be conducted. The results are summed up in Table 5 and are valid for weld clads made using:

(i) Voestalpine Böhler X70-IG Ø 1 mm wire
(ii) 18% CO2 in Argon shielding gas with a flow of 15 l/min
(iii) MIG CMT welding strategy
(iv) Torch travel speed of 0.6 m/min

Table 4 Wire feed measured internally by Fronius

Set wire feed	[m/min]	5.0	5.9	6.8	7.7	8.6
Measured average wire feed	[m/min]	5.6	6.6	7.4	7.9	8.5
Standard deviation	[m/min]	0.3	0.4	0.3	0.3	0.3

Table 5 Calibration results of basic parameters of the simplified model of the weld cladding

Weld clad	[-]	welding power 1	welding power 2	welding power 3	welding power 4	welding power 5
Set wire feed	[m/min]	5,0	5,9	6,8	7,7	8,6
Set current	[A]	127	146	155	162	176
Set voltage	[V]	15,4	16,4	16,8	17,1	17,4
Dw	[mm]	1	1	1	1	1
s	[m/min]	5,6	6,6	7,4	7,9	8,5
rw	[mm]	5,8	6,1	6,4	6,8	7,1
Ws	[%]	125	126	130	132	135
Wf	[-]	65	75	85	85	90

With these calibrated parameters, the simplified mathematical model of weld cladding could simulate weld clad that differs circa 0.20 mm and at the starting segments circa 0.30 mm from the real 3D scanned weld clads — see Figs. 16, 17, and 18. Coordinate systems synchronization was done as explained in Fig. 15. The side walls of the substrate plate were not machined so they are not fitting the ideal shape of the substrate from the simulation.

6 Conclusions

The aim of this study was to develop a simplified mathematical model of weld cladding which could predict weld clad position error. The simplified mathematical model of weld cladding was designed according to the physical phenomena affecting the weld clad position. Matlab software was used to create an interface for the simulation.

The simplified mathematical model contains variables describing the weld cladding behavior. In the study, values of these variables have been determined by an experimental calibration process where welded samples were 3D scanned and compared with the simulated weld clads.

For further calibration, weld pool parameters of the simplified model of weld cladding have to be investigated. For that

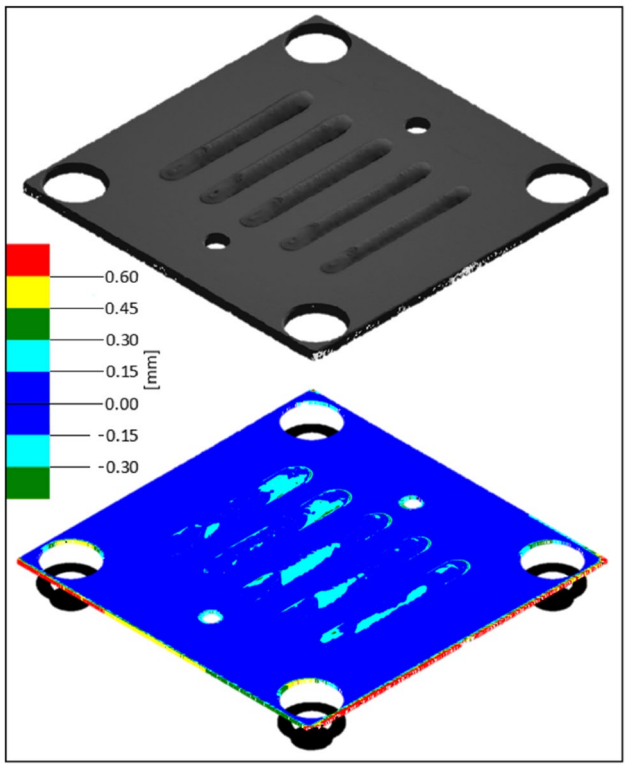

Fig. 17 Surface deviation between sample 2 and simulation

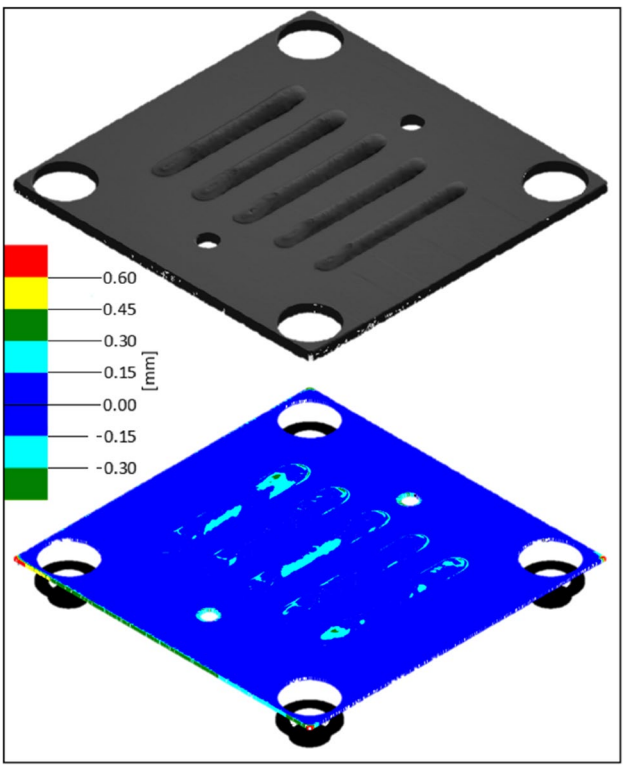

Fig. 16 Surface deviation between sample 1 and simulation

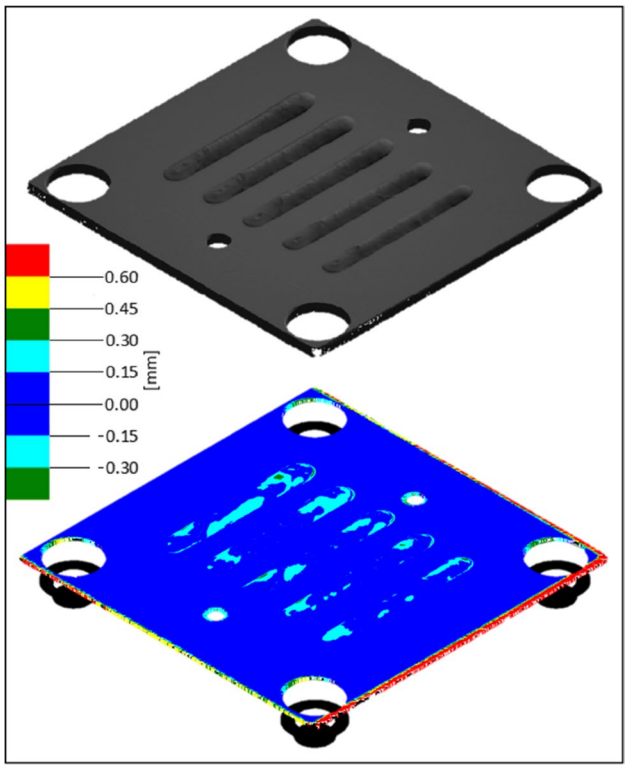

Fig. 18 Surface deviation between sample 3 and simulation

kind of calibration, experimental samples with curvaceous weld clads and substrates with geometrical elements will be necessary. These experiments will be the subject of further work.

In the current state, the simulation is able to predict the precise shape with a maximum deviation of circa 0.20 mm. The starts of weld clads is a more complex problem where the deviation is circa 0.30 mm. These are valuable results as the WAAM technology is generally considered to be reasonably rough. The simplified model is a promising method to predict position and shape errors of the WAAM weld clads. Further experiments with more complex toolpaths and substrate geometry will show if the simplification of the weld cladding was sufficiently accurate.

The simplified simulation model of the weld cladding will be extended with the function to recalculate the welding torch NC code toolpath based on the simulation results. These corrections will improve the weld clad position for some cases of the curved path weld clads. This function will also be the subject of further work and it is planned to validate it experimentally as well.

In this study, the knowledge of the WAAM process was improved in the field of weld pool and weld clad position by the simplified mathematical model of weld cladding that was developed and calibrated.

Acknowledgements Authors acknowledge support from the ESIF, EU Operational Programme Research, Development and Education, and from the Center of Advanced Aerospace Technology (CZ.02.1.01/0.0/0.0/16_019/0000826), Faculty of Mechanical Engineering, Czech Technical University in Prague. This work was also supported by the Grant Agency of the Czech Technical University in Prague, grant no. SGS22/159/OHK2/3T/12.

Author contribution Not applicable.

Funding Open access publishing supported by the National Technical Library in Prague.

Data Availability The authors confirm that the data and material supporting the findings of this work are available within the article.

Declarations

Ethics approval The article follows the guidelines of the Committee on Publication Ethics (COPE) and involves no studies on human or animal subjects.

Consent to participate Not applicable. The article involves no studies on humans.

Consent for publication Not applicable. The article involves no studies on humans.

Competing interests The authors declare no competing interests.

References

1. Acheson R (1990) Automatic welding apparatus for weld buildup and method of achieving weld build-up; US patent no. (4) 952–769 17
2. Williams SW, Martina F, Addison AC, Ding J, Pardal G, Colegrove P (2016) Wire + arc additive manufacturing. Mater Sci Technol 32(7):641–647. https://doi.org/10.1179/1743284715Y.0000000073
3. Moghadam M, Casalino G, Contuzzi N (2023) Metal wire additive manufacturing: a comparison between arc laser and laser/arc heat sources. Inventions 8:52. https://doi.org/10.3390/inventions8020052
4. Feldhausen T, Paramanathan M, Heineman J, Hassen AA, Heinrich L, Kurfess R, Fillingim B, Saleeby K, Post B (2023) Hybrid manufacturing of conformal cooling channels for tooling. J Manuf Mater Process 7:74. https://doi.org/10.3390/jmmp7020074
5. Rodrigues T, Duarte V, Miranda RM, Santos T, Oliveira JP (2019) Current status and perspectives on wire and arc additive manufacturing (WAAM). Materials 12:1121. https://doi.org/10.3390/ma12071121
6. Votruba V, Diviš I, Pilsová L et al (2022) Experimental investigation of CMT discontinuous wire arc additive manufacturing of Inconel 625. Int J Adv Manuf Technol 122:711–727. https://doi.org/10.1007/s00170-022-09878-7
7. Montevecchi F, Venturini G, Scippa A, Campatelli G (2016) Finite element modelling of wire-arc-additive-manufacturing process. Procedia CIRP 55:109–114. https://doi.org/10.1016/j.procir.2016.08.024
8. Saadlaoui Y, Feulvarch É, Delache A, Leblond J, Bergheau J (2018) A new strategy for the numerical modeling of a weld pool. Comptes Rendus Mécanique 346(11):999–1017. https://doi.org/10.1016/j.crme.2018.08.007
9. Xavier CR, Junio HG, Castro JA (2011) Numerical evaluation of the weldability of the low alloy ferritic steels T/P23 and T/P24. Mater Res 14(1):73–90. https://doi.org/10.1590/s1516-14392011005000019
10. Petrik J, Sydow B, Bambach M (2021) Beyond parabolic weld bead models: AI-based 3D reconstruction of weld beads under transient conditions in wire-arc additive manufacturing. J Mater Process Technol 302:117457. https://doi.org/10.1016/j.jmatprotec.2021.117457
11. Glasder M, Fabbri M, Aschwanden I, Bambach M, Wegener K (2023) Towards a general and numerically efficient deposition model for wire-arc directed energy deposition. Addit Manuf 78:103832. https://doi.org/10.1016/j.addma.2023.103832
12. Kučera D, Linkeová I, Stejskal M (2023) The influence of CAD model continuity on accuracy and productivity of CNC machining. Int J Adv Manuf Technol 124:1115–1128. https://doi.org/10.1007/s00170-022-10422-w
13. Cadiou S, Courtois M, Carin M, Berckmans W, P. Le masson, 3D heat transfer, fluid flow and electromagnetic model for cold metal transfer wire arc additive manufacturing (Cmt-Waam), Additive

Manufacturing, Volume 36, 2020, 101541, ISSN 2214–8604, https://doi.org/10.1016/j.addma.2020.101541.
14. https://www.fronius.com/en/welding-technology/world-of-welding/fronius-welding-processes/cmt. Accessed 26 June 2023
15. Kah P, Suoranta R, Martikainen J (2013) Advanced gas metal arc welding processes. Intl J Adv Manuf Technol 67:655–674. https://doi.org/10.1007/s00170-012-4513-5
16. Dzelnitzki D (1999) Increasing the deposition volume or the welding speed?—Advantages of heavy-duty MAG welding. Weld Cut 9:197–204
17. Kim C, Cho D-W, Kim S, Song S, Seo K, Cho YT (2022). High-throughput metal 3D printing pen enabled by a continuous molten droplet transfer. Adv Sci. 10. https://doi.org/10.1002/advs.202205085
18. Ríos S, Colegrove PA, Martina F, Williams SW (2018) Analytical process model for wire + arc additive manufacturing. Addit Manuf 21:651–657. https://doi.org/10.1016/j.addma.2018.04.003
19. Dou Z, Lyu F, Wang L, Gao C, Zhan X (2023) Relationship between droplet transfer and forming quality in wire arc additive manufacturing of 2319 aluminum alloy. Intl J Adv Manuf Technol. 129. https://doi.org/10.1007/s00170-023-11879-z
20. Felippa CA (2004) Introduction to finite element methods, University of Colorado at Boulder. (Available from: https://vulcanhammernet.files.wordpress.com/2017/01/ifem.pdf. Accessed 24 October 2023
21. Goldak J, Chakravarti A, Bibby M (1984) A new finite element model for welding heat sources. Metallurgical Transactions B [online]. 15(2), 299–305 [cit. 2018–07–22]. DOI: https://doi.org/10.1007/BF02667333
22. Hu Z, Qin X, Shao T, Liu H (2018) Understanding and overcoming of abnormity at start and end of the weld bead in additive manufacturing with GMAW. Intl J Adv Manuf Technol. 95. https://doi.org/10.1007/s00170-017-1392-9
23. Nguyen L, Buhl J, Bambach M (2020) Continuous Eulerian tool path strategies for wire-arc additive manufacturing of rib-web structures with machine-learning-based adaptive void filling. Addit Manuf 35:101265. https://doi.org/10.1016/j.addma.2020.101265
24. Viola R, Balandraud X, Poulhaon F, Michaud P, Duc E (2023) Complex interaction between CMT equipment and robot controllers during the WAAM process: consequences for toolpath accuracy. Intl J Adv Manuf Technol 127:1–21. https://doi.org/10.1007/s00170-023-11928-7
25. Wang X, Wang A, Li Y (2019) A sequential path-planning methodology for wire and arc additive manufacturing based on a water-pouring rule. Intl J Adv Manuf Technol. 103. https://doi.org/10.1007/s00170-019-03706-1